Chapter 6

On coupled systems of singularly perturbed Volterra integro-differential equations[5]

In this chapter, we consider the following system of singularly perturbed Volterra integro-differential equations (SPVIDEs)

$$\begin{cases} \mathcal{T}\mathbf{v} := \mathcal{E}\mathbf{v}'(t) + A(t)\mathbf{v}(t) + \displaystyle\int_0^t B(t,s)\mathbf{v}(s)\,ds = \mathbf{f}(t), \quad t \in \Omega, & (6.1) \\ \mathbf{v}(0) = \boldsymbol{\beta}, & (6.2) \end{cases}$$

where $\Omega = (0,1]$, $\mathbf{f}(t) = (f_1(t), f_2(t))^T$, $\mathbf{v}(t) = (v_1(t), v_2(t))^T$, and the given initial constant vector is $\boldsymbol{\beta} = (\beta_1, \beta_2)^T$. Also,

$$\mathcal{E} = \begin{pmatrix} \varepsilon_1 & 0 \\ 0 & \varepsilon_2 \end{pmatrix}, \quad A(t) = \begin{pmatrix} a_{11}(t) & a_{12}(t) \\ a_{21}(t) & a_{22}(t) \end{pmatrix}, \quad B(t,s) = \begin{pmatrix} b_{11}(t,s) & b_{12}(t,s) \\ b_{21}(t,s) & b_{22}(t,s) \end{pmatrix}.$$

Here, ε_1 and ε_2 are the two perturbation parameters ($0 < \varepsilon_1, \varepsilon_2 \ll 1$) which give rise to the singular behaviour of problem (6.1)–(6.2). The matrix-valued functions $A(t), \mathbf{f}(t) \in C^1(\overline{\Omega})$ and the kernel $B(t,s) \in C^1(\overline{\Omega} \times \mathbb{R})$ are assumed to be reasonably smooth. In addition, for each $i, j = 1, 2$, there exists some constants $\alpha_i, \beta_i, \bar{B}, \bar{B}_t$

[4]This chapter contains material published in *Computational and Applied Mathematics*, 42 (278), 2023, doi: `https://doi.org/10.1007/s40314-023-02406-7`.

and $\bar{B}_s$ such that

$$\begin{cases} a_{ii}(t) \geq \alpha_i > 0, \qquad a_{ij}(t) \leq 0, \quad i \neq j, \quad \forall\, t \in \overline{\Omega}, & (6.3) \\ \beta_i = \max\limits_{t \in \overline{\Omega}} |a_{ij}(t)|, \qquad i \neq j, & (6.4) \\ \bar{B} = \max\limits_{(t,s) \in \overline{\Omega} \times \overline{\Omega}} |B(t,s)|, \quad \bar{B}_t = \max\limits_{(t,s) \in \overline{\Omega} \times \overline{\Omega}} |B_t(t,s)|, \quad \bar{B}_s = \max\limits_{(t,s) \in \overline{\Omega} \times \overline{\Omega}} |B_s(t,s)|. & (6.5) \end{cases}$$

Here, B_t and B_s represent the partial derivatives of $B(t,s)$ with respect to t and s respectively. In 2020, Liang et al. [1] considered the system of SPVIDEs of the form (6.1)–(6.2). They discretized the problem by a finite difference scheme, which was proved stable under the condition $\alpha_k + \tau_j b_{kk}(t_j, t_j) \geq \alpha_{k*} > 0,\ 1 \leq j \leq N,\ k = 1, 2$, where τ_j denotes the mesh spacing. Further, the authors gave a posteriori error analysis and derived an a posteriori error estimate in the maximum norm. Unfortunately, there is a flaw in the a posteriori error estimation of [1] which we discuss here in detail and rectify this shortcoming.

In this chapter, our main objective is to propose a new finite difference scheme to discretize (6.1)–(6.2) that avoids the extra condition mentioned above. For our scheme, we obtain a posteriori error bound in L_∞ norm. Based on the obtained a posteriori error bound, an adaptive algorithm is tested and shown to produce first-order accurate results on the mesh constructed using the algorithm. Also, we conduct the a priori error analysis of our scheme.

The arrangement of this chapter is as follows. In Section 6.1, we mention the stability of continuous problem (6.1)–(6.2) and propose the discretization scheme. In Section 6.2, we perform the a priori error analysis of the discretization scheme. Section 6.3 covers the derivation of a posteriori error estimate for our scheme. Next, we present the correct a posteriori error estimation of [1] in Section 6.4. We perform some

numerical experiments n Section 6.5 that validate the theory. Finally, the chapter ends with the concluding remarks in Section 6.6.

6.1 Discretization

In this section, we propose the discretization scheme for the considered problem (6.1)–(6.2). Before we proceed further, we first provide an important lemma that will be helpful in deriving the a posteriori error bound in the subsequent section.

Lemma 6.1. *Under the problem hypotheses (6.3)–(6.5), the continuous solution* $\mathbf{v}$ *of the considered system (6.1)–(6.2) fulfills the following stability estimate*

$$\|\mathbf{v}\|_\infty \leq C\Big(\|\boldsymbol{\beta}\|_\infty + \|\mathbf{f}\|_\infty\Big). \tag{6.6}$$

Further, for any two function vectors $\mathbf{w}(t)$ *and* $\mathbf{z}(t)$ *such that* $\mathbf{w}(0) = \mathbf{z}(0)$ *and* $\mathfrak{T}\mathbf{w}(t) - \mathfrak{T}\mathbf{z}(t) = \mathfrak{G}(t)$*, where* $\mathfrak{G}(t)$ *is a bounded piecewise continuous function vector, we have*

$$\|\mathbf{w} - \mathbf{z}\|_\infty \leq C\|\mathfrak{T}\mathbf{w} - \mathfrak{T}\mathbf{z}\|_\infty. \tag{6.7}$$

Proof. See [1, Section 2]. □

Now, we construct an arbitrary non-uniform discretization grid $\overline{\Omega}^N \equiv \{0 = t_0 < t_1 < \cdots < t_N = 1\}$ such that $t_i = t_{i-1} + \tau_i$ for $1 \leq i \leq N$. Here, we denote τ_i as the mesh width and $\Omega^N = \{\overline{\Omega}^N \setminus 0\}$ as the set of interior mesh points. For any function w, we use the notation $w_i = w(t_i)$. Further, W_i represents the approximation of $w(t)$ at $t = t_i$. We define the backward Euler formula as

$$D^- W_i := \frac{W_i - W_{i-1}}{\tau_i}, \qquad \text{for } 1 \leq i \leq N,$$

where W is any mesh function.

In order to obtain the discretization scheme, we first integrate the considered problem (6.1) over the arbitrary interval (t_{i-1}, t_i) as follows

$$\mathcal{E}\int_{t_{i-1}}^{t_i}\mathbf{v}'(t)\,dt+\int_{t_{i-1}}^{t_i}A(t)\mathbf{v}(t)\,dt+\int_{t_{i-1}}^{t_i}\left(\int_0^t B(t,s)\mathbf{v}(s)\,ds\right)\,dt=\int_{t_{i-1}}^{t_i}\mathbf{f}(t)\,dt.$$

On applying the right-hand rectangle formula, we obtain

$$\mathcal{E}D^-\mathbf{v}_i+A_i\mathbf{v}_i+\int_0^{t_i}B(t_i,s)\mathbf{v}(s)\,ds+\mathfrak{R}_i^{(1)}=\mathbf{f}_i, \tag{6.8}$$

where

$$\mathfrak{R}_i^{(1)}=-\tau_i^{-1}\int_{t_{i-1}}^{t_i}(t-t_{i-1})\frac{d}{dt}\left(A(t)\mathbf{v}(t)+\int_0^t B(t,s)\mathbf{v}(s)\,ds-\mathbf{f}(t)\right)\,dt. \tag{6.9}$$

After incorporating the composite left-side rectangle rule to the integral term of (6.8), we arrive at

$$\mathcal{E}D^-\mathbf{v}_i+A_i\mathbf{v}_i+\sum_{m=1}^{i}\tau_m B(t_i,t_{m-1})\mathbf{v}_{m-1}+\mathfrak{R}_i=\mathbf{f}_i, \tag{6.10}$$

where

$$\begin{cases}\mathfrak{R}_i=\mathfrak{R}_i^{(1)}+\mathfrak{R}_i^{(2)}, & (6.11)\\ \mathfrak{R}_i^{(2)}=\displaystyle\sum_{m=1}^{i}\int_{t_{m-1}}^{t_m}(t_m-s)\frac{d}{ds}\left(B(t_i,s)\mathbf{v}(s)\right)ds. & (6.12)\end{cases}$$

Thereby, we finally propose the following discrete scheme corresponding to the continuous problem (6.1)–(6.2) after neglecting the truncation error term $\mathfrak{R}_i$:

$$\begin{cases} \mathfrak{T}^N \mathbf{V}_i := \mathcal{E} D^- \mathbf{V}_i + A_i \mathbf{V}_i + \sum_{m=1}^{i} \tau_m B(t_i, t_{m-1}) \mathbf{V}_{m-1} = \mathbf{f}_i, \quad i = 1, 2, \cdots, N, & (6.13) \\ \mathbf{V}_0 = \boldsymbol{\beta}, & (6.14) \end{cases}$$

where $\mathbf{V}_i = (V_{1,i}, V_{2,i})^T$ is the approximation of $\mathbf{v}(t)$ at $t = t_i$.

Remark 6.1. Note that the authors in [1] approximated the integral term of (6.8) by the composite right-side rectangle rule. So, in place of (6.13) they obtained $\mathcal{E} D^- \mathbf{V}_i + A_i \mathbf{V}_i + \sum_{m=1}^{i} \tau_m B(t_i, t_m) \mathbf{V}_m = \mathbf{f}_i,\ i = 1, 2, \cdots, N$, which was rewritten in [1, Section 4.1] as $\ell^N \mathbf{V}_i + \hat{K}_i \mathbf{V}_i + \sum_{m=1}^{i-1} \tau_m B(t_i, t_m) \mathbf{V}_m = \mathbf{f}_i,\ i = 1, 2, \cdots, N$, where $\ell^N \mathbf{V}_i := \mathcal{E} D^- \mathbf{V}_i + K_i \mathbf{V}_i$ with $K_i = \text{diag}(a_{11}(t_i) + \tau_i b_{11}(t_i, t_i), a_{22}(t_i) + \tau_i b_{22}(t_i, t_i))$ and $\hat{K}_i = \begin{pmatrix} 0 & a_{12}(t_i) + \tau_i b_{12}(t_i, t_i) \\ a_{21}(t_i) + \tau_i b_{21}(t_i, t_i) & 0 \end{pmatrix}$. The stability of the scheme was proved using a maximum principle for ℓ^N for which the assumption $\alpha_j + \tau_i b_{jj}(t_i, t_i) \geq \alpha_{j*} > 0, j = 1, 2,\ 1 \leq i \leq N$, was used. In order to avoid this condition, in the present chapter, we have applied the composite left-side rectangle rule to discretize the integral term of (6.8). For the present discrete scheme, we rewrite (6.13) as $\ell^N \mathbf{V}_i + \hat{K}_i \mathbf{V}_i + \sum_{m=1}^{i} \tau_m B(t_i, t_{m-1}) \mathbf{V}_{m-1} = \mathbf{f}_i$, where $\ell^N \mathbf{V}_i := \mathcal{E} D^- \mathbf{V}_i + K_i \mathbf{V}_i$ with $K_i = \text{diag}(a_{11}(t_i), a_{22}(t_i))$ and $\hat{K}_i = \begin{pmatrix} 0 & a_{12}(t_i) \\ a_{21}(t_i) & 0 \end{pmatrix}$. Clearly, the operator ℓ^N, for the present discrete scheme satisfies a maximum principle without any extra assumptions.

Now using the arguments in [1, Lemma 2] we can prove the following lemma.

Lemma 6.2. *The solution* $\mathbf{V}$ *of the discrete scheme (6.13)–(6.14) satisfies*

$$\|\mathbf{V}\|_{\overline{\Omega}^N} \leq C\Big(\|\boldsymbol{\beta}\|_{\overline{\Omega}^N} + \|\mathbf{f}\|_{\overline{\Omega}^N}\Big). \tag{6.15}$$

6.2 A priori error analysis

Let us define an error function $\boldsymbol{\phi} = \mathbf{V} - \mathbf{v}$ which satisfies the following error equation

$$\begin{cases} \mathcal{T}^N \boldsymbol{\phi}_i = \mathfrak{R}_i, \quad i = 1, 2, \cdots, N, \\ \boldsymbol{\phi}_0 = 0, \end{cases} \tag{6.16}$$

where the truncation error $\mathfrak{R}_i$ at nodal point t_i is given by (6.11). Thus, using Lemma 6.2, we get

$$\|\mathbf{v} - \mathbf{V}\|_{\overline{\Omega}^N} \leq C\|\mathfrak{R}\|_{\overline{\Omega}^N}. \tag{6.17}$$

Now, we bound the truncation error term $\mathfrak{R}_i$. For convenience, we calculate the bounds of $\mathfrak{R}_i^{(1)}$ and $\mathfrak{R}_i^{(2)}$ separately. From (6.9), we get

$$\begin{aligned} \left|\mathfrak{R}_i^{(1)}\right| &\leq \tau_i^{-1} \int_{t_{i-1}}^{t_i} |t - t_{i-1}| \left| \frac{d}{dt}\left(A(t)\mathbf{v}(t) + \int_0^t B(t,s)\mathbf{v}(s)\, ds - \mathbf{f}(t)\right)\right| dt \\ &\leq \int_{t_{i-1}}^{t_i} \left| A'(t)\mathbf{v}(t) + A(t)\mathbf{v}'(t) + B(t,t)\mathbf{v}(t) + \int_0^t \frac{\partial}{\partial t}\Big(B(t,s)\mathbf{v}(s)\Big)\, ds - \mathbf{f}'(t)\right| dt, \end{aligned}$$

where we have applied the Leibniz integral rule. Since the matrix-valued functions $A(t), B(t,s)$ and $\mathbf{f}(t)$ are sufficiently smooth therefore after taking (6.6) into the consideration we arrive at

$$\left|\mathfrak{R}_i^{(1)}\right| \leq C \int_{t_{i-1}}^{t_i} \left\{ \begin{pmatrix} 1 \\ 1 \end{pmatrix} + \begin{pmatrix} 1 & 1 \\ 1 & 1 \end{pmatrix} \begin{pmatrix} |v_1'(t)| \\ |v_2'(t)| \end{pmatrix} \right\} dt. \tag{6.18}$$

Similarly, from (6.12), we obtain

$$\begin{aligned}
\left|\mathfrak{R}_i^{(2)}\right| &\leq \sum_{m=1}^{i}\int_{t_{m-1}}^{t_m}|t_m-s|\left|\frac{d}{ds}\Big(B(t_i,s)\mathbf{v}(s)\Big)\right|ds\\
&= \sum_{m=1}^{i}\int_{t_{m-1}}^{t_m}|t_m-s|\left|B(t_i,s)\frac{d\mathbf{v}(s)}{ds}+\frac{dB(t_i,s)}{ds}\mathbf{v}(s)\right|ds\\
&\leq C\sum_{m=1}^{i}\tau_m\int_{t_{m-1}}^{t_m}\left\{\begin{pmatrix}1\\1\end{pmatrix}+\begin{pmatrix}1&1\\1&1\end{pmatrix}\begin{pmatrix}|v_1'(s)|\\|v_2'(s)|\end{pmatrix}\right\}ds\\
&\leq C\left(\max_{1\leq m\leq i}\int_{t_{m-1}}^{t_m}\left\{\begin{pmatrix}1\\1\end{pmatrix}+\begin{pmatrix}1&1\\1&1\end{pmatrix}\begin{pmatrix}|v_1'(s)|\\|v_2'(s)|\end{pmatrix}\right\}ds\right)\left(\sum_{m=1}^{i}\tau_m\right)\\
&\leq C\max_{1\leq m\leq i}\int_{t_{m-1}}^{t_m}\left\{\begin{pmatrix}1\\1\end{pmatrix}+\begin{pmatrix}1&1\\1&1\end{pmatrix}\begin{pmatrix}|v_1'(s)|\\|v_2'(s)|\end{pmatrix}\right\}ds. \qquad (6.19)
\end{aligned}$$

After combining the bounds obtained in (6.18) and (6.19), we have

$$|\mathfrak{R}_i|\leq C\max_{1\leq m\leq i}\int_{t_{m-1}}^{t_m}\left\{\begin{pmatrix}1\\1\end{pmatrix}+\begin{pmatrix}1&1\\1&1\end{pmatrix}\begin{pmatrix}|v_1'(s)|\\|v_2'(s)|\end{pmatrix}\right\}ds. \qquad (6.20)$$

Hence, using (6.17) and (6.20) we have the following a priori error bound.

Theorem 6.1. *Let* $\mathbf{v}$ *be the solution of (6.1)–(6.2) and* $\mathbf{V}$ *be its approximation by the finite difference scheme (6.13)–(6.14). Then, the following estimate holds*

$$\|\mathbf{v}-\mathbf{V}\|_{\overline{\Omega}^N}\leq C\max_{1\leq m\leq N}\int_{t_{m-1}}^{t_m}\left(1+\sum_{j=1}^{2}\left|v_j'(t)\right|\right)dt. \qquad (6.21)$$

Remark 6.2. Suppose the mesh is designed in a way that

$$\int_{t_{i-1}}^{t_i}\left(1+\sum_{j=1}^{2}\left|v_j'(t)\right|\right)dt=\frac{1}{N}\int_0^1\left(1+\sum_{j=1}^{2}\left|v_j'(t)\right|\right)dt$$

for $i = 1, \ldots, N$, and $\int_0^1 \left(1 + \sum_{j=1}^{2} \left|v_j'(t)\right|\right) dt \leq C$. Then, by Theorem 6.1, we obtain

$$\|\mathbf{v} - \mathbf{V}\|_{\overline{\Omega}^N} \leq CN^{-1}.$$

Thus, on this mesh first order uniform convergence of the proposed scheme can be achieved. However, constructing this mesh is not feasible because it necessitates having derivative bounds of $\mathbf{v}$ which are (generally) not available. When derivative bounds are available Theorem 6.1 can be employed to design meshes a priori; see Section 6.5. Consequently, in such circumstances, performing a posteriori error analysis is imperative as it does not necessitate any prior knowledge regarding the derivative bounds of the continuous solution.

6.3 A posteriori error analysis

In this section, we present a posteriori error analysis for the proposed discrete scheme (6.13)–(6.14). To this end, we assume that $\widetilde{\mathbf{V}}(t)$ is the piecewise linear interpolant vector function corresponding to the discrete solution vector $\{\mathbf{V}_i\}_{i=0}^N$. Therefore, $\widetilde{\mathbf{V}}(t)$ is continuous on $\overline{\Omega}$, linear on each interval $[t_{i-1}, t_i]$ and satisfies $\widetilde{\mathbf{V}}(t_i) = \mathbf{V}_i$, for $i = 0, 1, \cdots, N$. Further, for any $t \in [t_{i-1}, t_i]$, we have

$$\widetilde{\mathbf{V}}(t) = \mathbf{V}_i + (t - t_i)D^-\mathbf{V}_i, \qquad \text{and} \qquad \widetilde{\mathbf{V}}(t) = \mathbf{V}_{i-1} + (t - t_{i-1})D^-\mathbf{V}_i. \tag{6.22}$$

Theorem 6.2. *Let $\widetilde{\mathbf{V}}$ be the piecewise linear interpolant vector function corresponding to the solution vector $\mathbf{V}$ satisfying the discrete problem (6.13)–(6.14) on an*

arbitrary mesh $\{t_i\}_{i=0}^{N}$. *Suppose* $\mathbf{v}$ *is the continuous solution of the considered problem (6.1)–(6.2). Then*

$$\left\|\widetilde{\mathbf{V}}-\mathbf{v}\right\|_{\infty} \leq C \max_{1\leq i\leq N} \tau_i \left(1+\sum_{j=1}^{2}\left|D^{-}V_{j,i}\right|\right). \tag{6.23}$$

Proof. For any $t \in (t_{i-1}, t_i)$, we proceed for the proof by using (6.1) as follows

$$\begin{aligned}
\mathfrak{T}\widetilde{\mathbf{V}}(t)-\mathfrak{T}\mathbf{v}(t) &= \mathcal{E}[\widetilde{V}(t)]' + A(t)\widetilde{\mathbf{V}}(t) + \int_0^t B(t,s)\widetilde{\mathbf{V}}(s)\,ds - \mathbf{f}(t)\\
&= \mathcal{E}D^{-}\mathbf{V}_i + \left(A_i + \int_{t_i}^{t} A'(s)\,ds\right)\left(\mathbf{V}_i + (t-t_i)D^{-}\mathbf{V}_i\right)\\
&+ \sum_{m=1}^{i-1}\int_{t_{m-1}}^{t_m} B(t,s)\Big(\mathbf{V}_{m-1} + (t-t_{m-1})D^{-}\mathbf{V}_m\Big)\,ds\\
&+ \int_{t_{i-1}}^{t} B(t,s)\Big(\mathbf{V}_{i-1} + (t-t_{i-1})D^{-}\mathbf{V}_i\Big)\,ds - \left(\mathbf{f}_i + \int_{t_i}^{t}\mathbf{f}'(s)\,ds\right)\\
&= \mathcal{E}D^{-}\mathbf{V}_i + A_i\mathbf{V}_i + \sum_{m=1}^{i}\int_{t_{m-1}}^{t_m} B(t_i,t_{m-1})\mathbf{V}_{m-1}\,ds - \mathbf{f}_i\\
&+ A_i(t-t_i)D^{-}\mathbf{V}_i + \int_{t_i}^{t} A'(s)\,ds\,\mathbf{V}_i + (t-t_i)\int_{t_i}^{t} A'(s)\,ds\,D^{-}\mathbf{V}_i\\
&+ \sum_{m=1}^{i-1}\int_{t_{m-1}}^{t_m}\Big(B(t,s) - B(t_i,t_{m-1})\Big)\mathbf{V}_{m-1}\,ds\\
&+ \sum_{m=1}^{i-1}\int_{t_{m-1}}^{t_m}(t-t_{m-1})B(t,s)D^{-}\mathbf{V}_m\,ds + \int_{t_{i-1}}^{t}(t-t_{i-1})B(t,s)D^{-}\mathbf{V}_i\,ds\\
&+ \left(\int_{t_{i-1}}^{t} B(t,s)\,ds - \int_{t_{i-1}}^{t_i} B(t_i,t_{i-1})\,ds\right)\mathbf{V}_{i-1} - \int_{t_i}^{t}\mathbf{f}'(s)\,ds.
\end{aligned}$$

After taking (6.13) into account, we finally get

$$\begin{aligned}
\mathfrak{T}\widetilde{\mathbf{V}}(t)-\mathfrak{T}\mathbf{v}(t) &= A_i(t-t_i)D^{-}\mathbf{V}_i + \int_{t_i}^{t} A'(s)\,ds\,\mathbf{V}_i + (t-t_i)\int_{t_i}^{t} A'(s)\,ds\,D^{-}\mathbf{V}_i\\
&+ \sum_{m=1}^{i-1}\int_{t_{m-1}}^{t_m}\Big(B(t,s) - B(t_i,t_{m-1})\Big)\mathbf{V}_{m-1}\,ds
\end{aligned}$$

$$+\sum_{m=1}^{i-1}\int_{t_{m-1}}^{t_m}(t-t_{m-1})B(t,s)D^-\mathbf{V}_m\,ds+\int_{t_{i-1}}^{t}(t-t_{i-1})B(t,s)D^-\mathbf{V}_i\,ds$$
$$+\left(\int_{t_{i-1}}^{t}B(t,s)\,ds-\int_{t_{i-1}}^{t_i}B(t_i,t_{i-1})\,ds\right)\mathbf{V}_{i-1}-\int_{t_i}^{t}\mathbf{f}'(s)\,ds. \quad (6.24)$$

Now, we deal with each term of (6.24) separately. Incorporating Taylor expansion of $B(t,s)$ around the point (t_i,t_{m-1}) in the following expression, for some (η,ν) in between (t,s) and (t_i,t_{m-1}), we obtain

$$\begin{aligned}\left|\sum_{m=1}^{i-1}\int_{t_{m-1}}^{t_m}\Big(B(t,s)-B(t_i,t_{m-1})\Big)\mathbf{V}_{m-1}\,ds\right| &\le \sum_{m=1}^{i-1}\left|\int_{t_{m-1}}^{t_m}\mathbf{V}_{m-1}\Big(B(t_i,t_{m-1})+(t-t_i)\frac{\partial B}{\partial t}\Big|_{(\eta,\nu)}\right.\\ &\qquad\left.+(s-t_{m-1})\frac{\partial B}{\partial s}\Big|_{(\eta,\nu)}-B(t_i,t_{m-1})\Big)ds\right|\\ &\le \sum_{m=1}^{i-1}\Big(\bar{B}_t\tau_i+\bar{B}_s\tau_m\Big)|\mathbf{V}_{m-1}|\int_{t_{m-1}}^{t_m}ds\\ &\le C\max_{1\le m\le i}\tau_m\left(\sum_{m=1}^{i-1}\int_{t_{m-1}}^{t_m}ds\right)\begin{pmatrix}1\\1\end{pmatrix}\\ &\le C\max_{1\le m\le i}\tau_m\begin{pmatrix}1\\1\end{pmatrix}. \quad (6.25)\end{aligned}$$

We evaluate the next term as follows

$$\begin{aligned}&\left|\sum_{m=1}^{i-1}\int_{t_{m-1}}^{t_m}(t-t_{m-1})B(t,s)D^-\mathbf{V}_m\,ds+\int_{t_{i-1}}^{t}(t-t_{i-1})B(t,s)D^-\mathbf{V}_i\,ds\right|\\ &\qquad\le\sum_{m=1}^{i-1}\tau_m\bar{B}\big|D^-\mathbf{V}_m\big|\int_{t_{m-1}}^{t_m}ds+\tau_i\bar{B}\big|D^-\mathbf{V}_i\big|\int_{t_{i-1}}^{t}ds\\ &\qquad\le C\max_{1\le m\le i}\tau_m\begin{pmatrix}1&1\\1&1\end{pmatrix}\big|D^-\mathbf{V}_m\big|\left(\sum_{m=1}^{i-1}\int_{t_{m-1}}^{t_m}ds+\int_{t_{i-1}}^{t}ds\right)\\ &\qquad\le C\max_{1\le m\le i}\tau_m\begin{pmatrix}1&1\\1&1\end{pmatrix}\big|D^-\mathbf{V}_m\big|. \quad (6.26)\end{aligned}$$

Next, we have

$$\left|\left(\int_{t_{i-1}}^{t} B(t,s)\,ds - \int_{t_{i-1}}^{t_i} B(t_i,t_{i-1})\,ds\right)\mathbf{V}_{i-1}\right| \leq C\bar{B}\left(\int_{t_{i-1}}^{t} ds + \int_{t_i}^{t_{i-1}} ds\right)\begin{pmatrix}1\\1\end{pmatrix}$$
$$\leq C\tau_i\begin{pmatrix}1\\1\end{pmatrix}. \tag{6.27}$$

For the remaining terms, we obtain

$$\left|A_i(t-t_i)D^-\mathbf{V}_i + \int_{t_i}^{t} A'(s)\,ds\,\mathbf{V}_i + (t-t_i)\int_{t_i}^{t} A'(s)\,ds\,D^-\mathbf{V}_i - \int_{t_i}^{t}\mathbf{f}'(s)\,ds\right|$$
$$\leq C\tau_i\begin{pmatrix}1 & 1\\ 1 & 1\end{pmatrix}\left|D^-\mathbf{V}_i\right| + C\tau_i\begin{pmatrix}1\\1\end{pmatrix}. \tag{6.28}$$

Thus, after combining all these results from (6.25)–(6.28) in (6.24), we get

$$\left\|\mathfrak{T}\widetilde{\mathbf{V}}(t) - \mathfrak{T}\mathbf{v}(t)\right\|_\infty \leq C\max_{1\leq i\leq N}\tau_i\left(1+\sum_{j=1}^{2}\left|D^-V_{j,i}\right|\right).$$

Consequently, the desired estimate (6.23) can be obtained using (6.7). □

6.4 A posteriori error analysis for the discrete scheme of [1]

The main aim of this section is to present the correct a posteriori error analysis for the discrete scheme of [1]. For this purpose, we first mention the discrete scheme

considered in [1, Section 3] for the continuous problem (6.1)–(6.2):

$$\begin{cases} \mathcal{L}^N \mathbf{V}_i := \mathcal{E} D^- \mathbf{V}_i + A_i \mathbf{V}_i + \sum_{k=1}^{i} \tau_k B(t_i, t_k) \mathbf{V}_k = \mathbf{f}_i, \quad 1 \le i \le N, & (6.29) \\ \mathbf{V}_0 = \boldsymbol{\beta}. & (6.30) \end{cases}$$

One could obtain the first identity in the proof of [1, Theorem 1] only by using $\mathcal{E} D^- \mathbf{V}_i + A_i \mathbf{V}_i + \sum_{k=1}^{i} \int_{t_{k-1}}^{t_k} B(t_i, s) \mathbf{V}_k \, ds = \mathbf{f}_i$, which obviously does not hold true. The following theorem provides the correct a posteriori error estimation for the discrete scheme (6.29)–(6.30).

Theorem 6.3. *Let* $\mathbf{v} = (v_1, v_2(t))^T$ *be the solution of the continuous problem (6.1)–(6.2),* $\{\mathbf{V}_i\}_{i=0}^N$ *be the solution of the discrete problem (6.29)–(6.30) and* $\widetilde{\mathbf{V}}$ *be its piecewise linear interpolation vector as defined in (6.22). Then*

$$\left\| \widetilde{\mathbf{V}} - \mathbf{v} \right\|_\infty \le C \max_{1 \le i \le N} \tau_i \left(1 + \sum_{j=1}^{2} \left| D^- V_{j,i} \right| \right). \tag{6.31}$$

Proof. For $\forall\, t \in (t_{i-1}, t_i)$, we have

$$\begin{aligned} \mathfrak{T} \widetilde{\mathbf{V}}(t) - \mathfrak{T} \mathbf{v}(t) &= \mathcal{E} [\widetilde{\mathbf{V}}(t)]' + A(t) \widetilde{\mathbf{V}}(t) + \int_0^t B(t, s) \widetilde{\mathbf{V}}(s) \, ds - \mathbf{f}(t) \\ &= \mathcal{E} D^- \mathbf{V}_i + \left(A_i + \int_{t_i}^t A'(s) \, ds \right) \left(\mathbf{V}_i + (t - t_i) D^- \mathbf{V}_i \right) \\ &+ \sum_{k=1}^{i-1} \int_{t_{k-1}}^{t_k} B(t, s) \Big(\mathbf{V}_k + (t - t_k) D^- \mathbf{V}_k \Big) \, ds \qquad (6.32) \\ &+ \int_{t_{i-1}}^{t} B(t, s) \Big(\mathbf{V}_i + (t - t_i) D^- \mathbf{V}_i \Big) \, ds - \Big(\mathbf{f}(t) - \mathbf{f}_i + \mathbf{f}_i \Big) \\ &= \mathcal{E} D^- \mathbf{V}_i + A_i \mathbf{V}_i + \sum_{k=1}^{i} \int_{t_{k-1}}^{t_k} B(t_i, t_k) \mathbf{V}_k \, ds - \mathbf{f}_i \\ &+ A_i (t - t_i) D^- \mathbf{V}_i + \int_{t_i}^t A'(s) \, ds \, \mathbf{V}_i + (t - t_i) \int_{t_i}^t A'(s) \, ds \, D^- \mathbf{V}_i \end{aligned}$$

$$
\begin{aligned}
&+\sum_{k=1}^{i-1}\int_{t_{k-1}}^{t_k}\Big(B(t,s)-B(t_i,t_k)\Big)\mathbf{V}_k\,ds-\int_{t_{i-1}}^{t_i}B(t_i,t_i)\mathbf{V}_i\,ds\\
&+\sum_{k=1}^{i-1}\int_{t_{k-1}}^{t_k}B(t,s)(t-t_k)D^-\mathbf{V}_k\,ds+\int_{t_{i-1}}^{t}B(t,s)(t-t_i)D^-\mathbf{V}_i\,ds\\
&+\int_{t_{i-1}}^{t}B(t,s)\mathbf{V}_i\,ds-\Big(\mathbf{f}(t)-\mathbf{f}_i\Big)\\
&=A_i(t-t_i)D^-\mathbf{V}_i+\int_{t_i}^{t}A'(s)\,ds\,\mathbf{V}_i+(t-t_i)\int_{t_i}^{t}A'(s)\,ds\,D^-\mathbf{V}_i\\
&+\sum_{k=1}^{i-1}\int_{t_{k-1}}^{t_k}\Big(B(t,s)-B(t_i,t_k)\Big)\mathbf{V}_k\,ds-\int_{t_{i-1}}^{t_i}B(t_i,t_i)\mathbf{V}_i\,ds\\
&+\sum_{k=1}^{i-1}\int_{t_{k-1}}^{t_k}B(t,s)(t-t_k)D^-\mathbf{V}_k\,ds+\int_{t_{i-1}}^{t}B(t,s)(t-t_i)D^-\mathbf{V}_i\,ds\\
&+\int_{t_{i-1}}^{t}B(t,s)\mathbf{V}_i\,ds-\Big(\mathbf{f}(t)-\mathbf{f}_i\Big),
\end{aligned}
\tag{6.33}
$$

where we have used (6.29). Now we evaluate each terms of (6.32) separately. By Taylor expansions of $B(t,s)$ about (t_i,t_k) for some (ρ,ς) in between (t,s) and (t_i,t_k), it holds

$$
\begin{aligned}
\left|\sum_{k=1}^{i-1}\int_{t_{k-1}}^{t_k}\Big(B(t,s)-B(t_i,t_k)\Big)\mathbf{V}_k\,ds\right| &\le \sum_{k=1}^{i-1}\left|\int_{t_{k-1}}^{t_k}\Big(B(t_i,t_k)+(t-t_i)\frac{\partial B}{\partial t}\Big|_{(\rho,\varsigma)}\right.\\
&\qquad\left.+(s-t_k)\frac{\partial B}{\partial s}\Big|_{(\rho,\varsigma)}-B(t_i,t_k)\Big)\mathbf{V}_k\,ds\right|\\
&\le \sum_{k=1}^{i-1}\Big(\tau_i\bar{B}_t+\tau_k\bar{B}_s\Big)|\mathbf{V}_k|\int_{t_{k-1}}^{t_k}ds\\
&\le C\max_{1\le k\le i}\tau_k\left(\sum_{k=1}^{i-1}\int_{t_{k-1}}^{t_k}ds\right)\begin{pmatrix}1\\1\end{pmatrix}\\
&\le C\max_{1\le k\le i}\tau_k\begin{pmatrix}1\\1\end{pmatrix}.
\end{aligned}
\tag{6.34}
$$

Next, we use the arguments in Theorem 6.2 to obtain

$$\left|\sum_{k=1}^{i-1}\int_{t_{k-1}}^{t_k} B(t,s)(t-t_k)D^-\mathbf{V}_k\,ds+\int_{t_{i-1}}^{t} B(t,s)(t-t_i)D^-\mathbf{V}_i\,ds\right| \leq C\max_{1\leq k\leq i}\tau_k\begin{pmatrix}1 & 1\\ 1 & 1\end{pmatrix}\left|D^-\mathbf{V}_k\right|. \tag{6.35}$$

The rest of the terms can be estimated similar to Theorem 6.2. Thus, we obtain

$$\left\|\mathfrak{T}\widetilde{\mathbf{V}}(t)-\mathfrak{T}\mathbf{v}(t)\right\|_\infty \leq C\max_{1\leq i\leq N}\tau_i\left(1+\sum_{j=1}^{2}\left|D^-V_{j,i}\right|\right).$$

Hence, using (6.7), we finally get the desired result (6.31).

□

6.5 Numerical results

To solve the discrete system (6.13)–(6.14) on the a posteriori grid, we consider the a posteriori grid generating Algorithm 5 mainly due to De Boor [40]. Now, we provide the numerical findings based on the following example to validate the proposed theory.

Example 6.1. *We consider the system of SPVIDE of the form (6.1)–(6.2) having values*

$$A(t)=\begin{pmatrix}3 & -1\\ -2 & 3\end{pmatrix},\quad B(t,s)=\begin{pmatrix}2 & -1\\ 4 & -1\end{pmatrix},\quad \boldsymbol{\beta}=\begin{pmatrix}0\\ 0\end{pmatrix},$$

and $f_1(t)$ and $f_2(t)$ are chosen such that

$$v_1(t)=\frac{1-e^{-t/\varepsilon_1}}{1-e^{-1/\varepsilon_1}}+\frac{1-e^{-t/\varepsilon_2}}{1-e^{-1/\varepsilon_2}}-2\sin\left(\frac{\pi}{2}t\right),$$

Algorithm 5: A posteriori grid generating algorithm

Step 1. Initially assign $r = 0$ as the number of iterations and construct an arbitrary uniform mesh $\{t_i^{(r)} = i/N,\ 0 \le i \le N\}$.

Step 2. Define the mesh width $\tau_i^{(r)} = t_i^{(r)} - t_{i-1}^{(r)}$ for $1 \le i \le N$. Solve the discrete system (6.13)–(6.14) on the given mesh $\{t_i^{(r)}\}$, and store the solution $\{\mathbf{V}_i^{(r)},\ 0 \le i \le N\}$.

Step 3. Evaluate the following discrete monitor function chosen from the a posteriori estimate (6.23):

$$\mathcal{M}_i^{(r)} = 1 + \sum_{j=1}^{2} \left| D^- V_{j,i}^{(r)} \right|, \quad i = 1, 2, \cdots, N.$$

Compute $L_j^{(r)} = \sum_{i=1}^{j} \tau_i^{(r)} \mathcal{M}_i^{(r)}$ for $1 \le j \le N$ and set $L_0^{(r)} = 0$.

Step 4. Assign $\gamma = N \cdot \left(\max_{1 \le i \le N} \tau_i^{(r)} \mathcal{M}_i^{(r)} \right) / L_N^{(r)}$. For a user chosen constant $\gamma_0 \ge 1$, if the stopping criterion $\gamma \le \gamma_0$ is met, then jump to 6, else proceed to 5.

Step 5. Assume $Y_i = i \cdot L_N^{(r)}/N,\ 0 \le i \le N$. Using piecewise linear interpolation, interpolate the points $\left(Y_i^{(r)}, t_i^{(r+1)}\right)$ to $\left(L_i^{(r)}, t_i^{(r)}\right)$ for each $i = 0, 1, \cdots, N$. Thus, the new mesh $\left\{t_i^{(r+1)}\right\}_{i=0}^{N}$ is uniquely determined. Return to 2 with $r = r + 1$.

Step 6. Set $t^* := \left\{0 = t_0^* < t_1^* < \cdots < t_N^* = 1\right\} = \left\{t_i^{(r)}\right\}_{i=0}^{N}$ as the final a posteriori grid and $\mathbf{V}^* = \left\{\mathbf{V}_i^{(r)}\right\}_{i=0}^{N}$ as the final solution. *Stop.*

$$v_2(t) = \frac{1 - e^{-t/\varepsilon_2}}{1 - e^{-1/\varepsilon_2}} - te^{t-1}.$$

One expects the solution of problem (6.1)–(6.2) to exhibit overlapping layers near $t = 0$. Also, the derivative of $\mathbf{v}$ (for $\varepsilon_1 \le \varepsilon_2$) is expected to satisfy

$$|v_2'(t)| \le C\left\{1 + \frac{1}{\varepsilon_2} e^{-\alpha_2 t/\varepsilon_2}\right\}, \quad |v_1'(t)| \le C\left\{1 + \frac{1}{\varepsilon_1} e^{-\alpha_1 t/\varepsilon_1} + \frac{1}{\varepsilon_2} e^{-\alpha_2 t/\varepsilon_2}\right\}. \quad (6.36)$$

However, despite the authors' attempts, providing a proof for this assertion has thus far proven unsuccessful.

Bakhvalov meshes are constructed by equidistributing the monitor function given by

$$\mathcal{M}(t) := \max\left\{1, \frac{r_1}{\varepsilon_1}e^{-\alpha_1 t/\theta\varepsilon_1}, \frac{r_2}{\varepsilon_2}e^{-\alpha_2 t/\theta\varepsilon_2}\right\},$$

where r_1, r_2 and θ are user-chosen positive constants. Thus, the selection of mesh points is carried out in a manner such that

$$\int_0^{t_i} \mathcal{M}(t)\,dt = \frac{i}{N}\int_0^1 \mathcal{M}(t)\,dt, \quad i = 1, \cdots, N.$$

If (6.36) holds, then $|v_i'(t)| \leq C\mathcal{M}(t)$, $i = 1, 2$, $t \in \overline{\Omega}$, cf. [10]. Since $\displaystyle\int_0^1 \mathcal{M}(t)\,dt \leq C$, from Theorem 6.1, we get

$$\|\mathbf{v} - \mathbf{V}\|_{\overline{\Omega}^N} \leq CN^{-1}, \quad \text{if} \quad \theta \geq 1.$$

Shishkin meshes are constructed with the help of transition parameters σ_1 and σ_2 defined by

$$\sigma_2 = \min\left\{\frac{1}{2}, \frac{\varepsilon_2}{\alpha_1}\ln N\right\}, \qquad \sigma_1 = \min\left\{\frac{1}{4}, \frac{\sigma_2}{2}, \frac{\varepsilon_1}{\alpha_2}\ln N\right\}.$$

Suppose N is divisible by 4. Then, dividing the intervals $[0, \sigma_1], [\sigma_1, \sigma_2]$ and $[\sigma_2, 1]$ into $N/4, N/4$ and $N/2$ subintervals of equal widths, respectively, the mesh is constructed. If (6.36) holds true, then Theorem 6.1 gives

$$\|\mathbf{v} - \mathbf{V}\|_{\overline{\Omega}^N} \leq CN^{-1}\ln N,$$

	Number of intervals					
$\varepsilon_1 = 10^{-\kappa}$	$N = 2^6$	$N = 2^7$	$N = 2^8$	$N = 2^9$	$N = 2^{10}$	$N = 2^{11}$
$\kappa = 1$	1.2059e-01	6.5164e-02	3.8303e-02	2.1036e-02	1.0942e-02	5.7123e-03
	0.8880	0.7666	0.8646	0.9429	0.9377	
$\kappa = 2$	1.8035e-01	8.4597e-02	4.1590e-02	2.3982e-02	1.2524e-02	7.1846e-03
	1.0921	1.0244	0.7943	0.9372	0.80175	
$\kappa = 3$	1.7568e-01	8.6352e-02	4.6782e-02	2.2874e-02	1.2007e-02	6.2524e-03
	1.0247	0.8842	1.0323	0.9298	0.9413	
$\kappa = 4$	1.1088e-01	5.9962e-02	3.1695e-02	1.5717e-02	8.0471e-03	4.0555e-03
	0.8868	0.9198	1.0119	0.9658	0.9885	
$\kappa = 5$	5.0213e-02	2.5739e-02	1.2982e-02	6.5894e-03	3.3365e-03	1.6746e-03
	0.9641	0.9874	0.9783	0.9818	0.9946	
$\kappa = 6$	1.6967e-02	8.6769e-03	4.1378e-03	2.1904e-03	1.1240e-03	5.6505e-04
	0.9675	1.0683	0.9177	0.9626	0.9922	

TABLE 6.1: Maximum errors and the corresponding convergence rates on the posteriori grid for Example 6.1 taking $\varepsilon_2 = 10^{-6}$.

cf. [10].

In the experiment that follows, we compute the maximum errors and the convergence rates by the following formulas

$$E^N_{\varepsilon_1,\varepsilon_2} = \max_{j=1,2}\left\{\max_{0\le i\le N}|V_{j,i} - v_j(t_i)|\right\}, \quad \varrho^N_{\varepsilon_1,\varepsilon_2} = \log_2\left(\frac{E^N_{\varepsilon_1,\varepsilon_2}}{E^{2N}_{\varepsilon_1,\varepsilon_2}}\right),$$

while the uniform errors and the corresponding convergence rates are calculated by

$$E^N = \max_{\varepsilon_1,\varepsilon_2\in S}\left\{E^N_{\varepsilon_1,\varepsilon_2}\right\}, \quad \varrho^N = \log_2\left(\frac{E^N}{E^{2N}}\right),$$

where $S = \{(\varepsilon_1,\varepsilon_2)\,|\,\varepsilon_2 = 10^{-1},\ldots,10^{-6},\varepsilon_1 = \varepsilon_2,\ldots,10^{-8}\}$.

In order to generate the a posteriori grid, we set $\gamma_0 = 1.5$ throughout the experiment. We solve Example 6.1 for various values of N and report the maximum errors and the corresponding convergence rates in the tabular form. Table 6.1 displays the numerical results fixing $\varepsilon_2 = 10^{-6}$ and varying ε_1, while in Table 6.2 the results are

	Number of intervals					
$\varepsilon_2 = 10^{-\kappa}$	$N = 2^6$	$N = 2^7$	$N = 2^8$	$N = 2^9$	$N = 2^{10}$	$N = 2^{11}$
$\kappa = 1$	1.2690e-02	6.5029e-03	3.3775e-03	1.6419e-03	8.4400e-04	4.2603e-04
	0.9645	0.9452	1.0406	0.9600	0.9863	
$\kappa = 2$	1.5931e-02	8.1565e-03	4.2732e-03	2.0772e-03	1.0665e-03	5.3926e-04
	0.9658	0.9326	1.0407	0.9617	0.9839	
$\kappa = 3$	1.6297e-02	8.3271e-03	4.3723e-03	2.1620e-03	1.1056e-03	5.5674e-04
	0.9689	0.9294	1.0161	0.9675	0.9897	
$\kappa = 4$	1.5580e-02	8.0726e-03	4.3290e-03	2.0861e-03	1.0563e-03	5.4558e-04
	0.9486	0.8990	1.0532	0.9818	0.9531	
$\kappa = 5$	1.4632e-02	7.3362e-03	3.6917e-03	1.8460e-03	9.2367e-04	4.6222e-04
	0.9961	0.9907	0.9999	0.9989	0.9988	
$\kappa = 6$	1.6968e-02	8.6770e-03	4.1380e-03	2.1905e-03	1.1241e-03	5.6514e-04
	0.9675	1.0683	0.9177	0.9625	0.9921	

TABLE 6.2: Maximum errors and the corresponding convergence rates on the posteriori grid for Example 6.1 taking $\varepsilon_1 = 10^{-6}$.

presented fixing $\varepsilon_1 = 10^{-6}$ and varying ε_2. In this way, we have shown the numerical results on a posteriori meshes for all possible ordering of ε_1 and ε_2. It is evident from the results that the method is first-order convergent irrespective of the parameters ε_1 and ε_2. Further, we also compare the uniform errors and the corresponding rates of convergence on a priori and a posteriori meshes for Example 6.1, which is shown in Table 6.3.

N	Shishkin mesh		Bakhvalov mesh		A Posteriori mesh	
	E^N	ϱ^N	E^N	ϱ^N	ϱ^N	E^N
2^6	1.1018e-01	0.5679	9.8834e-02	1.0740	1.0946e-01	0.7697
2^7	7.4327e-02	0.6358	4.6947e-02	0.9839	6.4205e-02	1.0184
2^8	4.7837e-02	0.6839	2.3737e-02	0.9793	3.1696e-02	1.0093
2^9	2.9777e-02	0.7149	1.2040e-02	0.9937	1.5746e-02	0.9516
2^{10}	1.8142e-02	0.7327	6.0465e-03	0.9883	8.1413e-03	1.0139
2^{11}	1.0917e-02	–	3.0479e-03	–	4.0317e-03	–

TABLE 6.3: Comparison of uniform errors and uniform convergence rates on various meshes for Example 6.1.

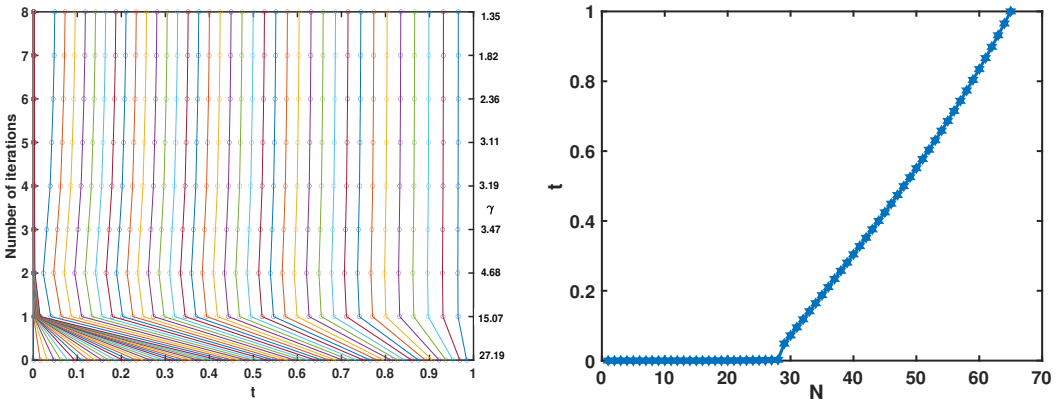

(A) Mesh trajectory (B) Mesh position

FIGURE 6.1: Mesh points movement at each iteration and the mesh position for $\varepsilon_1 = 10^{-3}, \varepsilon_2 = 10^{-7}$ and $N = 64$.

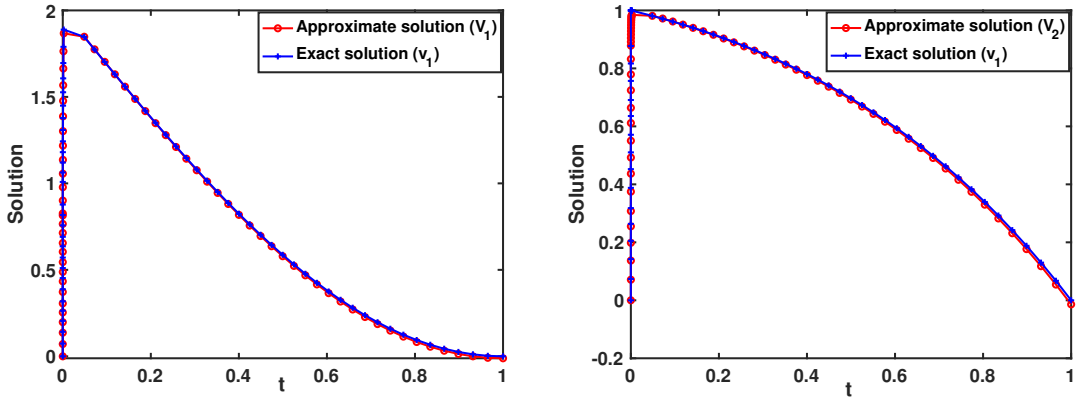

(A) First solution component (B) Second solution component

FIGURE 6.2: Comparison of solution plots for $\varepsilon_1 = 10^{-3}, \varepsilon_2 = 10^{-7}$ and $N = 64$.

Figure 6.1A depicts the mesh movement throughout each iteration of the a posteriori grid, whereas Figure 6.1B displays the final computed mesh when $\varepsilon_1 = 10^{-3}, \varepsilon_2 = 10^{-7}$ and $N = 64$. Additionally, the value of constant γ at each iteration is also displayed on the right side of the Figure 6.1A which clearly shows the adaptive nature of the a posteriori grid. Finally, we graphically compare the approximate solution and the exact solution for each component in Figure 6.2 for $\varepsilon_1 = 10^{-3}, \varepsilon_2 = 10^{-7}$ and $N = 64$. One can observe from Figures 6.2A and 6.2B that there is an overlapping layer near $t = 0$, and the plots of approximate solutions are in alignment with the

plot of exact solutions for both components.

6.6 Conclusions

A system of singularly perturbed Volterra integro-differential equations with initial conditions, characterized by overlapping layers, has been considered. The discretization of the problem is accomplished using the backward Euler formula for the differential component, and the integral term is approximated using the left-hand rectangle rule. Both a priori and a posteriori error analysis are conducted for the discrete scheme proposed in this chapter. The a posteriori error bound is then used to generate a grid adaptively, effectively resolving the layer phenomena. Furthermore, the correct a posteriori error estimate for the discrete scheme introduced in [1] is also presented. Finally, numerical experiments are carried out to validate the theory.